DOI 10.1007/s11595-017-1577-y

Influence of Different Chelating Agents on Corrosion Performance of Microstructured Hydroxyapatite Coatings on AZ91D Magnesium Alloy

ZHAO Dandan, SUN Ruixue*, CHEN Kezheng

(College of Materials Science and Engineering, Qingdao University of Science and Technology, Qingdao 266042, China)

Abstract: To improve the bioactivity and corrosion resistance of AZ91D magnesium alloy, hydroxyapatite (HAp) coatings with novel microstructured morphologies were prepared successfully on AZ91D substrates via a facile hydrothermal method. Different chelating agents including polyaspartic acid (PASP) and ethylenediaminetetraacetic acid (EDTA) were introduced to investigate their effects on the morphology and corrosion resistance of the coated magnesium alloys. The results revealed that the coating prepared with PASP was composed of many uniform urchin-like microspheres, while the coating prepared with EDTA consisted of many flower-like particles. Moreover, the crystallinity of the coating prepared with EDTA was much higher than that of the coating prepared with PASP. Electrochemical tests revealed that the corrosion resistance of the substrate was significantly improved after being coated with each coating. Immersion test of the coated samples in simulated body fluid (SBF) demonstrated that the coatings could be biodegraded gradually and induce the formation of calcium phosphate particles.

Key words: magnesium alloy; hydroxyapatite coating; chelating agent; corrosion resistance

1 Introduction

Metallic implants such as stainless steels, titanium and its alloys as well as cobalt-chromium-based alloys have been widely used to repair or replace damaged load-bearing bones in clinical applications[1]. The limitations of these metallic implants involve the stress-shielding effects, the requirement for second surgeries, and the release of toxic ions[2]. Magnesium and its alloys are regarded as next-generation biodegradable metallic implants because of their good biocompatibility, bone-like mechanical properties and gradual degradation in physiological media[3-6]. Unfortunately, the rapid corrosion rate and high hydrogen evolution of magnesium alloys in the human physiological environment limit their clinical applications. Thus, the present key challenge of using magnesium alloys is in controlling their degradation to a reasonably low rate. Constructing protective bioceramic coatings has been considered as the simplest way to improve the corrosion resistance and bioactivity of magnesium alloys[7-10].

Hydroxyapatite (HAp, $Ca_{10}(PO_4)_6(OH)_2$) is the main inorganic component of bone and has been considered as an excellent coating material for orthopedic implants due to its excellent biocompatibility, bioactivity, and high corrosion resistance[11-13]. A number of methods, including biomimetic methods, electrodeposition (ED), plasma spraying, micro-arc oxidation, and hydrothermal method have been applied to deposit HAp coatings on magnesium alloys[14-19]. Among these methods, hydrothermal treatment is a promising method owing to its simple set up, cost-effectiveness and low temperature requirement[1]. In addition, the morphology and crystallinity of the coating can be controlled easily by controlling the hydrothermal parameters. However, few attempts have been made so far to prepare HAp coating on magnesium alloy by hydrothermal method. This is because direct synthesis of HAp on magnesium alloy in aqueous solution is difficult due to the prevention of HAp crystallization by Mg ions[20]. Hiromoto *et al* prepared HAp coatings on pure

(Received: Oct. 20, 2015; Accepted: Nov. 4, 2016)

ZHAO Dandan (赵丹丹): E-mail: 1697011174@qq.com

*Corresponding author: SUN Ruixue (孙瑞雪): Assoc. Prof.; Ph D; E-mail: sunruixue@qust.edu.cn

Funded by Shandong Provincial Natural Science Foundation, China (No. ZR2014EMM019)

magnesium and magnesium alloys by a single-step hydrothermal treatment using an aqueous Ca-EDTA solution[21]. It was revealed that the HAp coating can effectively improve the corrosion resistance and apatite formation ability of magnesium alloy. Moreover, the authors pointed out that the success in HAp direct synthesis relied on Ca-EDTA (chelating agent) which enabled the surface of the substrate to maintain a high concentration of Ca ions to overcome the prevention of HAp crystallization by Mg ions[21]. Ohtsu *et al* also reported the HAp and octacalcium phosphate (OCP) coatings deposited on Mg substrate through using the same chelating agent (Ca-EDTA)[22]. Consequently, the chelating agent used in hydrothermal method plays an important role in determining the morphology and crystallinity of the HAp coating. However, very limited work has been reported on the effects of different chelating agents on properties of the prepared coatings.

In the present study, two different chelating agents (PASP and EDTA) were employed to produce HAp coating on AZ91D magnesium alloy through using a hydrothermal method. The influence of the used chelating agents on the morphology and anticorrosion properties of the prepared coatings was investigated. The corrosion resistance and in vitro corrosion behavior of the coated samples were evaluated by electrochemical experiments and immersion tests in simulated body fluid (SBF).

2 Experimental

2.1 Coating preparation

All the chemicals used in this work were analytical grade and without any further purification. Commercial AZ91D magnesium alloys (8.64 wt% Al, 0.592 wt% Zn, 0.261 wt% Mn and balance Mg) with dimension of 16 mm× 14 mm× 6 mm were used as the substrate materials. The substrate was ground progressively to 2000 grits by using silicon carbide abrasive paper, and then degreased with acetone, ultrasonically rinsed in distilled water and dried in warm air. A treatment solution was prepared with calcium chloride ($CaCl_2$), PASP (or EDTA-2Na), and potaussium dihydrogen phosphate (KH_2PO_4). The concentrations of $CaCl_2$ and KH_2PO_4 were 100 and 60 mmol/L, respectively. For the coating prepared with PASP, 0.25 g PASP was dissolved in 20 mL NaOH solution and then mixed with 20 mL $CaCl_2$ solution with vigorous stirring. For the coating prepared with EDTA, 0.60 g EDTA-2Na was dissolved in 50 mL deionized water and then mixed with 20 mL $CaCl_2$ solution with vigorous stirring. The pre-treated samples were immersed in the above two solutions at room temperature for 15 min, respectively. Then, 20 mL KH_2PO_4 solution was added drop-wise to the above solutions. The pH of the solutions was adjusted to 5.0 using a diluted HCl (100 mmol/L) solution. Finally, the samples were placed in a Teflon container and the solution was also transferred into this container, which was placed in an oven at 95 ℃ for 10 h. After the heat-treatment, the samples were taken out of the container and rinsed in running water followed by warm air drying.

2.2 Characterization of the coating

The surface morphologies of the coated samples were observed by a field emission-scanning electron microscope (FE-SEM, JEOL, JSM-6700F) equipped with an energy dispersive spectrometer (EDS). The phase composition of the coated samples was analyzed by X-ray diffraction (XRD, Rigaku, D/max-2500) using a Cu Kα radiation. Diffraction patterns were generated between 2θ of 10-70º, with a step increment of 0.04º and a scanning speed of 4º/min. Infared spectroscopic analyses were conducted on the coated samples in the range of 4 000-600 cm^{-1} by using attenuated total reflection-Fourier transform infrared spectroscopy (ATR-FTIR, Bruker, Tensor 27) with a resolution of 4.0 cm^{-1}.

2.3 Electrochemical measurement

The electrochemical measurements were performed on an electrochemical workstation (CS380, China) in SBF at 36.5±0.5 ℃. SBF was composed of 8.0 g/L NaCl, 0.35 g/L $NaHCO_3$, 0.4 g/L KCl, 0.23 g/L $K_2HPO_4{\cdot}3H_2O$, 0.31 g/L $MgCl_2{\cdot}6H_2O$, 0.14 g/L $CaCl_2$, 0.07 g/L Na_2SO_4, 6.12 g/L Tris and pH=7.4. A classical three electrodes cell with platinum as counter electrode, saturated calomel electrode SCE as reference electrode and the samples as working electrode was used for the measurements. The samples were allowed to stabilize at their open circuit potential (OCP) for 10 min before the measurements were started. The potentiodynamic polarization tests were conducted at a scan rate of 0.8 mV/s in a scan range of ±250 mV with reference to OCP. The electrochemical impedance spectra were collected over a frequency range from 0.01 Hz to 100 kHz.

2.4 Immersion experiment

The immersion tests were carried out to investigate the degradation and the corrosion resistance of the coated samples in SBF solution at 36.5±0.5 ℃

for various durations. And bare AZ91D alloys were immersed under the same condition to be compared with the coated ones. The volume of solution was obtained based on a volume-to-surface area ratio of 20 mL/cm^2, according to ASTM G31-72[23]. The SBF solution was refreshed every day. After different periods of time, the samples were removed from the SBF solution, rinsed in distilled water and air dried overnight for surface examination.

3 Results and discussion

3.1 Microstructure and composition of coatings

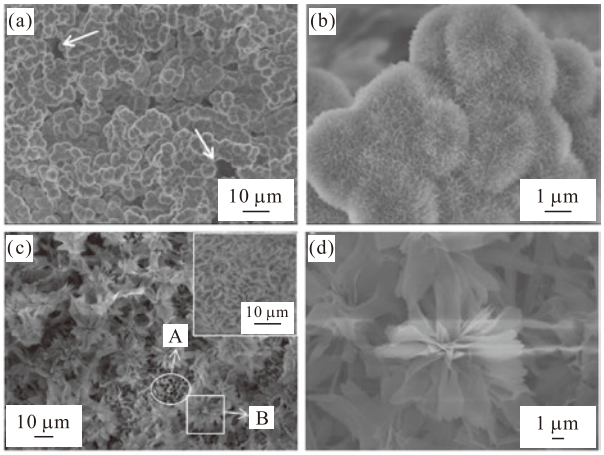

Fig.1 Surface morphologies of (a), (b) the coating prepared with PASP; (c) the coating prepared with EDTA (the inset is the high magnification of region A); and (d) high magnification of region B shown in (c)

Surface morphologies of the coatings prepared with PASP and EDTA were observed by FESEM in Fig.1. It is evident that these two coatings show different surface morphologies. It can be seen from Fig. 1a that large quantities of microspheres with the diameter of 1-2 μm densely covered the coating surface prepared with PASP. Further observation from the SEM image (Fig.1(b)) indicated that the microspheres had an urchin-like shape and connected closely with each other. This kind of urchin-like microsphere densely and uniformly covered the surface without apparent microcracks. But the coating was not complete, with some micro-pores between the microspheres (marked by arrows in Fig.1(a)). The coating prepared with EDTA (Fig.1(c)) showed layer by layer growth mode with some microflowers covering the outer surface. The microflower with the size of 10-15 μm as shown in Fig.1(d) was composed of many nano-plates with various sizes. The inner layer of the coating (inset in Fig.1(c)) exhibited a flake-like microstructure with flakes of 1-2 μm in length and interconnected with each other without preferred growth direction. Both of these two coatings had a rough surface due to the micro-structured building units, which might be a favor for the bone tissue to infiltrate into the implants and thus accelerate the healing of the damaged bone[24, 25].

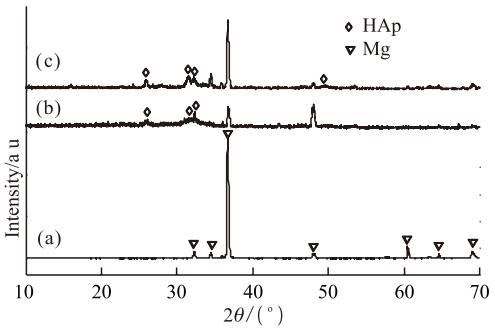

Fig.2 XRD patterns of (a) uncoated, (b) the coating prepared with PASP, and (c) the coating prepared with EDTA

The XRD patterns of the two coatings prepared with PASP and EDTA as well as the uncoated substrate are shown in Fig.2. It can be seen from Fig.2 that the diffraction peaks of HAp were detected in both coatings in addition to the diffraction peaks from the magnesium alloy substrate. Compared with the coating prepared with PASP, HAp phase in the coating prepared with EDTA had much higher crystallinity. Moreover, the amorphous phase was also present in both coatings, especially in the coating prepared with PASP. No other phases such as tricalcium phosphate ($Ca_3(PO_4)_2$) and magnesium phosphate ($Mg_3(PO_4)_2$) as reported by other researches[20,26] were detected in both coatings.

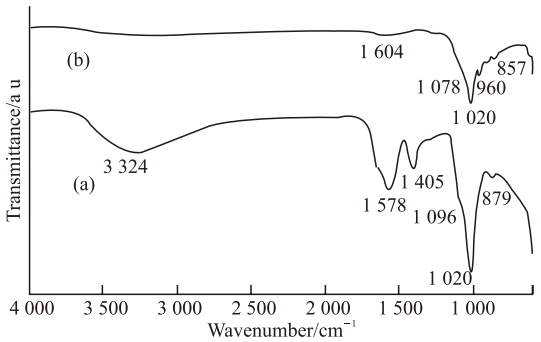

Fig.3 ATR-FTIR spectra of (a) the coating prepared with PASP and (b) the coating prepared with EDTA

Fig.3 shows the FTIR spectra of the two prepared coatings. The broad band at 3 324 cm^{-1} in Fig.3(a) is attributed to H_2O in the coating. The bands at 1 020, 1 078 and 1 096 cm^{-1} are assigned to the v_3 P-O asymmetric stretching. The v_1 symmetric P-O stretching band is observed at 960 cm^{-1} in Fig.3(b). Some authors pointed out that the degree of HAp crystallinity can be derived from the intensity of the P-O

stretching band at 960 cm^{-1}[27,28]. Therefore, it can be concluded that HAp phase in the coating prepared with EDTA has much higher crystallinity than that in the coating prepared with PASP, which is also consistent with the XRD result. No bands in the range of 560-610 cm^{-1} corresponding to O-P-O bending appeared in the spectra because the measurement ranges of ATR-FTIR used in this study was 4 000-600 cm^{-1}. The weak absorption bands at 879 and 857 cm^{-1} are attributed to the presence of CO_3^{2-} in the coatings, which may originate from the atmosphere during the process. In addition, the FTIR spectra also show the bands corresponding to the organic functional group of COO^- at 1 604, 1 578, and 1 405 cm^{-1}[29, 30], suggesting that the chelating agents remained in the two coatings. As it can be observed, much more PASP than EDTA remained in the prepared coatings, which could be due to the lower solubility of PASP in water.

3.2 Formation mechanism of coatings

It is difficult to directly form pure HAp coatings on magnesium and its alloys through a hydrothermal method, because high hydrothermal temperature can cause heavy corrosion of Mg and the released Mg^{2+} may substitute Ca^{2+} in the structure of the coatings[1]. In this study, two Ca chelating agents were used to achieve a high concentration of Ca^{2+} on the substrate surface and thus induce the rapid formation of HAp layer. Based on the experimental results obtained in this study and some other studies[20,31], the formation mechanism of the HAp coating prepared with EDTA was schematically illustrated in Fig.4.

The following corrosion reaction occurs immediately after immersing the substrate in the treatment solution at pH 5.0:

$$Mg \rightarrow Mg^{2+} + 2e^- \quad (1)$$

$$2H_2O + 2e^- \rightarrow H_2 + 2OH^- \quad (2)$$

The hydrogen generation reaction raises the pH on the substrate surface rapidly with rapid corrosion of the substrate. At the same time, Ca^{2+} ions in the solution can react with EDTA to form Ca-EDTA complex, leading to a high concentration of Ca^{2+} ions on the substrate surface. The pH increase and the high concentration of Ca^{2+} ions initiate the rapid nucleation of HAp on the substrate surface (Fig.4(b)), which can separate the substrate from the treatment solution and prevent the subsequent release of Mg^{2+} ions. As shown in the inset image in Fig.4(b), the first precipitate layer consisted of many dome-shaped particles as reported by other researchers[31]. In the latter stage of the hydrothermal treatment, new layer of HAp particles with flower-like morphology formed and covered the initially precipitated layer (Fig.4(c)). The formation of $Mg(OH)_2$ was not found in the two coatings prepared in this study. It is probably because the solubility of HAp in H_2O is much lower than that of $Mg(OH)_2$[31]. On the other hand, the high concentration of Ca^{2+} on the substrate surface due to the chelating agents is in favor of the rapid formation of HAp.

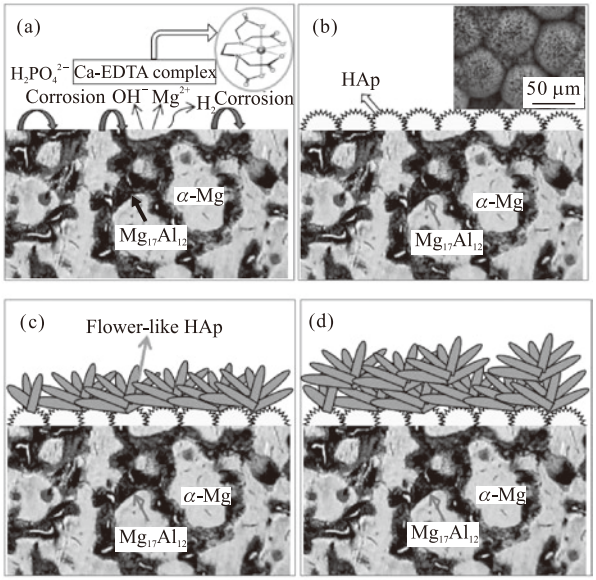

Fig.4 Schematic diagram of the formation mechanism of HAp coating prepared with EDTA on AZ91D alloy

For the coating prepared with PASP, the same formation mechanism can also be applied. PASP is a polyelectrolyte with –COOH and $–NH_2$ terminals, which also has a high binding ability with Ca^{2+} to form Ca-PASP complex[29]. The difference is the morphology of the coatings, which could be due to the different chemical structures and functional groups of the two chelating agents. The detailed relationship between the morphology of the coating and the chelating agent still need to be studied. To further identify the effect of PASP on the formation of HAp coating, some control experiments were also carried out without PASP while other conditions remained unchanged. The results show that only some white precipitates formed on the substrate and a continuous layer of coating cannot be achieved without PASP. This also proves that the chelating agent plays an important role in the formation of the HAp coating on AZ91D alloy.

3.3 Corrosion resistance

To evaluate the corrosion resistance of the two prepared coatings, potentiodynamic polarization and EIS tests were conducted for these coatings as well as

uncoated samples. Fig.5 shows the polarization curves of different samples in SBF. The corrosion potential (E_{corr}) and the corrosion current density (I_{corr}) are extracted from the polarization curves via Tafel region extrapolation and the values of these parameters are summarized in Table1. It is well known that the coating with high corrosion potential and low corrosion current density is usually considered to have a low corrosion rate and provides a good corrosion resistance[19]. From Fig.5 and Table 1, it can be noticed that the uncoated substrate has a low corrosion potential (−1.692 V) and a high corrosion current density (3.002×10^{-4} A/cm^2). After the surface is modified by coatings, the E_{corr} of the samples shifts to the positive direction of −1.572 and −1.419 V for the coating prepared with PASP and EDTA, respectively. Besides, a significant decrease of I_{corr} from 3.002×10^{-4} A/cm^2 to 3.033×10^{-6} A/cm^2 is achieved under the protection of the coating prepared with EDTA.

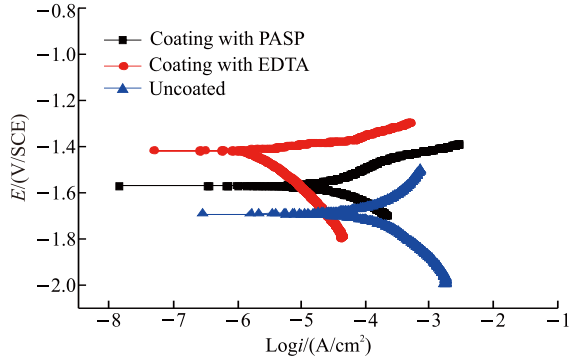

Fig.5 Potentiodynamic polarization curves of the coatings and the uncoated substrate in SBF

Table 1 Electrochemical parameters of polarization curves

Samples	E_{corr}/(V/SCE)	I_{corr}/(A/cm^2)
Uncoated substrate	−1.692	3.002×10^{-4}
Coating with PASP	−1.572	3.859×10^{-5}
Coating with EDTA	−1.419	3.033×10^{-6}

The corresponding Nyquist plots in Fig.6 further characterize the electrochemical behavior of the samples in SBF. It can be seen from Fig.6 that the high frequency capacitive loop of the three samples can be associated with the electrical double layer at the interface of the electrolyte solution[26]. The low frequency inductance loops of the uncoated substrate and the coating prepared with EDTA may be attributed to the breakdown of the surface coating or relaxation of the adsorbed species. As for the coating prepared with PASP, two capacitive loops appeared at high and low frequencies, indicating that corrosion has begun during the test process. It is well known that the charge transfer resistance, *i e*, the diameter of the capacitive loop in Nyquist plots, represents the polarization resistance of the tested samples. The uncoated substrate has a polarization resistance of 900 Ω·cm^2, showing the worst corrosion resistance among the three samples. The values of the coatings prepared with PASP and EDTA are approximately 2 100 Ω·cm^2 and 3 400 Ω·cm^2, respectively. It is clear that the coating prepared with EDTA shows better anti-corrosion performance than that of the uncoated substrate and the coating prepared with PASP. This result is in agreement with the polarization curve results shown in Fig.5 and Table 1. Amorphous or less crystalline HAp phases have been found to be more soluble and thus have a high dissolution rate in body fluids[32]. It can be seen from the results of XRD and FTIR that the crystallinity of the coating prepared with EDTA is much higher than that of the coating prepared with PASP, which may be one of the reasons to lead to the better anti-corrosion property of the coating prepared with EDTA.

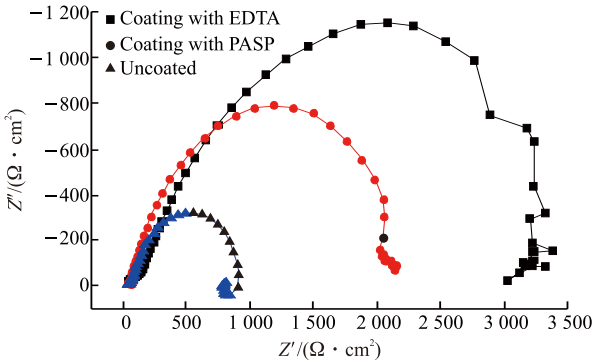

Fig.6 EIS plots of the coatings and the uncoated substrate in SBF

3.4 Immersion test

In order to further evaluate the biocorrosion resistance and the apatite formation ability, the samples were immersed in SBF for different periods. Fig.7 reveals the morphologies of the samples after different immersion times. After being immersed for 1 day (Fig.7(a)), the coating prepared with PASP did not show much difference compared to the one before immersion (Fig.1(b)). With increasing immersion time to 5 days, some sphere-like particles were deposited homogeneously on the urchin-like microspheres. But the original microspheres can still be clearly observed. After 8 days of immersion, the precipitates can be clearly seen on the microspheres (Fig.7(c)). When the coating prepared with EDTA is immersed in SBF for 5 days (Fig.7(e)), the contour of the microflowers becomes ambiguous and irregular due to the dissolution of the coating. With increasing

immersion time, the building units of the microflowers gradually dissolved into small chippings (Fig.7(f)). But no obvious precipitates were detected on the immersed coating prepared with EDTA. This could be due to the lower dissolution rate in SBF compared with that of the coating prepared with PASP.

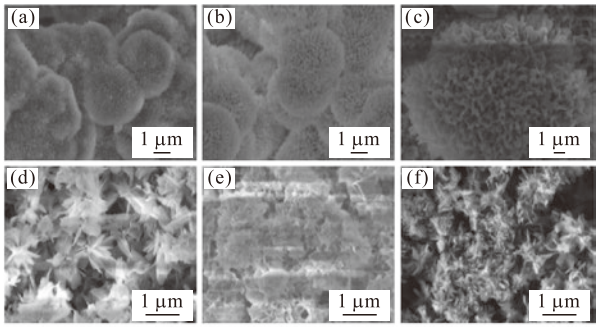

Fig.7 Surface morphologies of the coatings prepared with PASP (a-c) and EDTA (d-e) after immersed in SBF solution for (a, d) 1 day, (b, e) 5 days, and (c, f) 8 days

To further verify the composition of the precipitates, the content of elements in immersed coatings as shown in Table 2 was extracted through EDS analysis. It can be seen from Table 2 that the immersed coatings are mainly composed of Ca, P, Mg, and O. Although the coating itself consists of Ca and P, the concentration of Ca and P increased with increasing immersion time, suggesting that the coatings could induce the deposition of calcium phosphate particles through dissolution of themselves. The Ca/P atomic ratio of the samples after immersed for 8 days is 1.41, which is close to that of hydroxyapatite (1.67). However, the contents of calcium and phosphate in the sample prepared with PASP are higher than those in the sample prepared with EDTA.

Table 2 Elemental composition of the coatings after immersed in SBF for different days/at%

Element	Coating with PASP		Coating with EDTA	
	5 days	8 days	5 days	8 days
Ca	14.84	22.50	16.29	18.60
P	13.13	15.95	13.03	13.18
O	70.28	59.59	69.67	67.44
Mg	1.75	1.96	1.02	0.78

The change of surface morphology as well as the content of Ca and P elements indicated that the coating can be biodegraded gradually and induce the formation of calcium phosphate particles. Moreover, no large crack formation was observed on the surface of both coatings during the whole immersion test. The remaining coating can continue to provide protection to the substrates.

4 Conclusions

In this study, two microstructured hydroxyapatite coatings prepared on AZ91D magnesium alloys through using two different chelating agents were comparatively investigated. The chelating agents play an important role in determining the morphology and corrosion resistance of the prepared coatings. EIS and potentiodynamic polarization tests prove that the two prepared coatings both can greatly improve the corrosion resistance of the substrates. But the coating prepared with EDTA shows better anti-corrosion performance compared to the coating prepared with PASP. The immersion tests in SBF demonstrate that the prepared coatings are biodegradable and can induce the precipitation of calcium phosphate particles. Further studies of the corrosion mechanism of the coated samples in SBF should be performed in future.

References

[1] Dorozhkin S V. Calcium Orthophosphate Coatings on Magnesium and Its Biodegradable Alloys [J]. *Acta Biomater*., 2014, 10(7): 2 919-2 934

[2] Sonmez S, Aksakal B, Dikici B. Influence of Hydroxyapatite Coating Thickness and Powder Particle Size on Corrosion Performance of MA8M Magnesium Alloy[J]. *J. Alloys Comp*., 2014, 596(5): 125-131

[3] Cui W, Beniash E, Gawalt E, *et al*. Biomimetic Coating of Magnesium Alloy for Enhanced Corrosion Resistance and Calcium Phosphate Deposition[J]. *Acta Biomater.*, 2013, 9(10): 8 650-8 659

[4] Hornberger H, Virtanen S, Boccaccini A R. Biomedical Coatings on Magnesium Alloys-A Review[J]. *Acta Biomater*., 2012, 8(7): 2 442-2 455

[5] Shadanbaz S, Dias G J. Calcium Phosphate Coatings on Magnesium Alloys for Biomedical Applications: A Review[J]. *Acta Biomater*., 2012, 8(1): 20-30

[6] Li N, Zheng Y F. Novel Magnesium Alloys Developed for Biomedical Application: A Review [J]. *J. Mater. Sci. Technol.*, 2013, 29(6): 489-502

[7] Zheng Y F, Gu X N, Witte F. Biodegradable Metals[J]. *Mater. Sci. Eng. R*, 2014, 77(2):1-34

[8] Rudd A L, Breslin C B, Mansfeld F. The Corrosion Protection Afforded by Rare Earth Conversion Coatings Applied to Magnesium[J]. *Corros. Sci.*, 2000, 42(2): 275-278

[9] Shi Z M, Song G L, Atrens A. The Corrosion Performance of Anodised Magnesium Alloys[J]. *Corros. Sci.*, 2006, 48(11): 3 531-3 546

[10] Ambrt R, Zhou W. Electroless Nickel-plating on AZ91D Magnesium Alloy: Effect of Substrate Microstructure and Plating Parameters[J]. *Surf. Coat. Technol.*, 2004, 179(2-3): 124-134

[11] Noorakma Abdullah C W, Zuhailawati H, Aishvarya V, *et al*. Hydroxyapatite-Coated Magnesium-Based Biodegradable Alloy: Cold Spray Deposition and Simulated Body Fluid Studies[J]. *J. Mater. Eng.*

Perform., 2013, 22(10): 2 997-3 004

[12] Singh S S, Roy A, Lee B, *et al*. Aqueous Deposition of Calcium Phosphates and Silicate Substituted Calcium Phosphates on Magnesium Alloys[J]. *Mater. Sci. Eng. B*, 2011, 176(20): 1 695-1 702

[13] Lin X, Wang X, Tan L L, *et al.* Effect of Preparation Parameters on the Properties of Hydroxyapatite Containing Micro-arc Oxidation Coating on Biodegradable ZK60 Magnesium Alloy[J]. *Ceram. Int*., 2014, 40(7): 10 043-10 051

[14] Su Y C, Li G Y, Lian J S. A Chemical Conversion Hydroxyapatite Coating on AZ60 Magnesium Alloy and Its Electrochemical Corrosion Behavior[J]. *Int. J. Electrochem. Sci*., 2012, 7(11): 11 497-11 511

[15] Ma X, Zhu S J, Wang L G, *et al*. Synthesis and Properties of a Bio-composite Coating Formed on Magnesium Alloy by One-step Method of Micro-arc Oxidation[J]. *J. Alloys Comp*., 2014, 590(2): 247-253

[16] Yanovska A, Kuznetsov V, Stanislavov A, *et al*. Calcium-Phosphate Coatings Obtained Biomimetically on Magnesium Substrates Under Low Magnetic Field[J]. *Appl. Surf. Sci*., 2012, 258(22): 8 577-8 584

[17] Xu L P, Zhang E L, Yang K. Biocorrosion Property and Cytocompatibility of Calcium Phosphate Coated Mg Alloy[J]. *Trans. Nonferrous Met. Soc. China*, 2012, 22(8): 2 014-2 020

[18] Wang B, Huang P, Ou C W, *et al. In Vitro* Corrosion and Cytocompatibility of ZK60 Magnesium Alloy Coated with Hydroxyapatite by a Simple Chemical Conversion Process for Orthopedic Applications[J]. *Int. J. Mol. Sci*., 2013, 14(12): 23 614-23 628

[19] Tang H, Yu D Z, Luo Y, *et al*. Preparation and Characterization of HA Microflowers Coating on AZ31 Magnesium Alloy by Micro-arc Oxidation and A Solution Treatment[J]. *Appl. Surf. Sci.*, 2013, 264(1): 816-822

[20] Hiromoto S, Yamamoto A. High Corrosion Resistance of Magnesium Coated with Hydroxyapatite Directly Synthesized in An Aqueous Solution[J]. *Electrochim. Acta*, 2009, 54(27): 7 085-7 093

[21] Hiromoto S, Tomozawa M. Corrosion Behavior of Magnesium with Hydroxyapatite Coatings Formed by Hydrothermal Treatment[J]. *Mater. Trans*., 2010, 51(11): 2 080-2 087

[22] Ohtsu N, Hiromoto S, Yamane M, *et al.* Chemical and Crystallographic Characterizations of Hydroxyapatite- and Octacalcium Phosphate-Coatings on Magnesium Synthesized by Chemical Solution Deposition Using XPS and XRD[J]. *Surf. Coat. Technol*., 2013, 218(218):114-118

[23] ASTM Standards. *Standard Practice for Laboratory Immersion Corrosion Testing of Metals*[S]. ASTM Standard G31-72, 2004

[24] Park J H, Lee Y K, Kim K M. Bioactive Calcium Phosphate Coating Prepared on H_2O_2-Treated Titanium Substrate by Electrodeposition[J]. *Surf. Coat. Technol*., 2005, 195(2-3): 252-257

[25] Song Y W, Shan D Y, Han E H. Electrodeposition of Hydroxyapatite Coating on AZ91D Magnesium Alloy for Biomaterial Application[J]. *Mater. Lett.*, 2008, 62(17-18): 3 276-3 279

[26] Song Y W, Shan D Y, Han E H. A Novel Biodegradable Nicotinic Acid/calcium Phosphate Composite Coating on Mg-3Zn Alloy[J]. *Mater. Sci. Eng. C*, 2013, 33(1):78-84

[27] Lak A, Mazloumi M, Mohajerani M, *et al.* Self-Assembly of Dandelion-Like Hydroxyapatite Nanostructures via Hydrothermal Method[J]. *J. Am. Ceram. Soc*., 2008, 91(10): 3 292-3 297

[28] Rameshbabu N, Rao K P, Kumar T S S. Accelerated Microwave Processing of Nanocrystalline Hydroxyapatite[J]. *J. Mater. Sci*., 2005, 40(23): 6 319-6 323

[29] Jiang S D, Yao Q Z, Zhou G T, *et al.* Fabrication of Hydroxyapatite Hierarchical Hollow Microspheres and Potential Application in Water Treatment[J]. *J. Phys. Chem. C*, 2012, 47(116): 4 484-4 492

[30] Kolodynska D, Hubicki Z, Geca M. Polyaspartic Acid as A New Complexing Agent in Removal of Heavy Metal Ions on Polystyrene Anion Exchangers[J]. *Ind. Eng. Chem. Res*., 2008, 47(6): 6 221-6 227

[31] Tomozawa M, Hiromoto S. Growth Mechanism of Hydroxyapatite-Coatings Formed on Pure Magnesium and Corrosion Behavior of the Coated Magnesium[J]. *Appl. Surf. Sci*., 2011, 257(19): 8 253-8 257

[32] Surmenev R A, Surmeneva M A, Ivanova A A. Significance of Calcium Phosphate Coatings for the Enhancement of New Bone Osteogenesis – A Review[J]. *Acta Biomater*., 2014, 10(2): 557-579